

## Non-uniformity effects in the negative effective magnetic pressure instability

This article has been downloaded from IOPscience. Please scroll down to see the full text article.

2013 Phys. Scr. 2013 014027

(<http://iopscience.iop.org/1402-4896/2013/T155/014027>)

View [the table of contents for this issue](#), or go to the [journal homepage](#) for more

Download details:

IP Address: 130.225.213.198

The article was downloaded on 20/07/2013 at 04:57

Please note that [terms and conditions apply](#).

# Non-uniformity effects in the negative effective magnetic pressure instability

K Kemel<sup>1,2</sup>, A Brandenburg<sup>1,2</sup>, N Kleeorin<sup>1,3</sup> and I Rogachevskii<sup>1,3</sup>

<sup>1</sup> NORDITA, Roslagstullsbacken 23, SE-10691 Stockholm, Sweden

<sup>2</sup> Department of Astronomy, Stockholm University, SE-10691 Stockholm, Sweden

<sup>3</sup> Department of Mechanical Engineering, Ben-Gurion University of the Negev, PO Box 653, Beer-Sheva 84105, Israel

E-mail: [koen@nordita.org](mailto:koen@nordita.org)

Received 9 August 2012

Accepted for publication 2 October 2012

Published 16 July 2013

Online at [stacks.iop.org/PhysScr/T155/014027](http://stacks.iop.org/PhysScr/T155/014027)

## Abstract

In direct numerical simulations of strongly stratified turbulence we have previously studied the development of large scale magnetic structures starting from a uniform background field. This is caused by an instability resulting from a negative contribution of small-scale turbulence to the effective (mean-field) magnetic pressure, and was qualitatively reproduced in mean-field simulations (MFS) where this pressure reduction was modeled as a function of the mean magnetic field normalized by the equipartition field. We now investigate the effect of mean current density on the turbulent pressure reduction. In our MFS, such currents are associated with sharp gradients of the growing structures. We find that an enhanced mean current density increases the suppression of the turbulent pressure.

PACS numbers: 91.25.Cw, 92.60.hk, 94.05.Lk, 96.50.Tf, 96.60.qd

(Some figures may appear in color only in the online journal)

## 1. Introduction

The Sun's magnetic field is generally believed to be due to a turbulent dynamo operating in the convection zone, the outer 30% by radius (Moffatt 1978, Parker 1979, Krause and Rädler 1980, Zeldovich *et al* 1983, Brandenburg and Subramanian 2005). Recent simulations performed by a number of groups indicated that the magnetic field is produced in the bulk of the convection zone. According to the flux tube scenario, most of the toroidal magnetic field resides at the bottom of the convection zone, or possibly just beneath it (Gilman and Dikpati 2000, Parfrey and Menou 2007). Another possibility is that most of the toroidal field resides in the bulk of the convection zone, but that its spatio-temporal properties are strongly affected by the near-surface dynamics (Käpylä *et al* 2012a), or the near-surface shear layer (Brandenburg 2005). In any case, the question then emerges how one can explain the formation of active regions out of which sunspots develop during the lifetime of an active region.

In the past, this question was conveniently bypassed by referring to the possible presence of a strong toroidal

flux belt at the bottom of the convection zone, where they would be in a stable state, except that every now and then they would become unstable, for example the clamshell or tipping instabilities (Cally *et al* 2003). However, if the magnetic field is continuously being destroyed and regenerated by the turbulence in the convection zone proper, the mechanism for producing active regions and eventually sunspots must be one that is able to operate within a turbulent environment. One such mechanism may be the negative effective magnetic pressure instability (NEMPI) which is based on the suppression of turbulent pressure by a weak mean magnetic field, leading therefore to a negative *effective* (or mean-field) magnetic pressure and, under suitable conditions, to an instability (Kleeorin *et al* 1989, 1990, 1993, 1996, Kleeorin and Rogachevskii 1994, Rogachevskii and Kleeorin 2007). This has been the subject of intensive research in recent years (Brandenburg *et al* 2010, 2012, Käpylä *et al* 2012b, Kemel *et al* 2012a, 2012b, 2012c, Losada *et al* 2012), following the first detection of such an instability in direct numerical simulations (DNS; see Brandenburg *et al* 2011). Another mechanism that has been discussed in connection with the production of magnetic

flux concentrations is related to the suppression of the turbulent convective heat flux (Kitchatinov and Mazur 2000). Meanwhile, simulations of realistic solar convection have demonstrated that large-scale magnetic flux inhomogeneities can develop when horizontal magnetic flux is injected at the bottom of the simulation domain (Stein and Nordlund 2012), but it remains to be seen whether this is connected with any of the two aforementioned mechanisms.

The purpose of the present paper is to investigate the possibility that higher-order contributions (involving spatial derivatives of the mean magnetic field) might play a role in NEMPI. We do this by using DNS to measure the resulting turbulent transport coefficients in cases where a measurable mean current density develops in the DNS. Note that even for an initially uniform mean magnetic field, a mean current density develops as a consequence of NEMPI itself, which redistributes an initially uniform magnetic field into a structured one. Our mean-field simulations (MFS) show that indeed the spatial variations of the magnetic field may become quite large as the instability runs further into saturation. We begin by first discussing the basic equations and turn then to the simulation results. Note that throughout this work we use an isothermal equation of state, which yields the simplest possible system to investigate this process. It is interesting that, while in mixing length theory turbulence is generally thought of as destructive, here, in the presence of gravity and a mean magnetic field, turbulence is found to actually drive a large-scale constructive mechanism. The resulting instability can be described in the general mean-field framework, with, notably, very good agreement with the DNS results.

## 2. Basic equations

In this paper we use both DNS and MFS to study the effects of non-uniformity of the magnetic field due to the development of NEMPI. In the DNS a two-dimensional pattern emerges, which can best be isolated using averaging over the  $y$ -direction. By imposing a uniform magnetic field, we can determine some of the turbulent transport coefficients that characterize the dependence of the Reynolds and Maxwell stress on the mean field. This is generally done by determining the total mean stress

$$\overline{\Pi}_{ij} = \overline{\rho U_i U_j} + \frac{1}{2} \delta_{ij} \overline{\mathbf{B}^2} - \overline{B_i B_j}. \quad (1)$$

Here, the vacuum permeability is set to unity and overbars indicate  $y$  averages. This total mean stress has contributions from the fluctuations,

$$\overline{\Pi}_{ij}^f = \overline{\rho u_i u_j} + \frac{1}{2} \delta_{ij} \overline{\mathbf{b}^2} - \overline{b_i b_j}, \quad (2)$$

where  $\mathbf{u} = \mathbf{U} - \overline{\mathbf{U}}$  and  $\mathbf{b} = \mathbf{B} - \overline{\mathbf{B}}$  are the departures from the averaged fields. Here  $\overline{\mathbf{U}}$  and  $\overline{\mathbf{B}}$  are the mean velocity and magnetic fields, and  $\overline{\rho}$  is the mean fluid pressure. This, together with the contribution from the mean fields, namely

$$\overline{\Pi}_{ij}^m = \overline{\rho U_i U_j} + \delta_{ij} \left( \overline{p} + \frac{1}{2} \overline{\mathbf{B}^2} \right) - \overline{B_i B_j} - 2\nu \overline{\rho S_{ij}}, \quad (3)$$

yields the total mean stress tensor, i.e.  $\overline{\Pi}_{ij} = \overline{\Pi}_{ij}^m + \overline{\Pi}_{ij}^f$ . The term  $\overline{\Pi}_{ij}^m$  depends only on the mean field and is therefore directly obtained in MFS, while  $\overline{\Pi}_{ij}^f$  is caused by

the fluctuating velocity and magnetic fields and requires a parameterization. It has a contribution independent of the mean field,  $\overline{\Pi}_{ij}^{f,0}$ , and one that depends on it,  $\Delta \overline{\Pi}_{ij}^f(\overline{\mathbf{B}})$ . Much of the recent work in this field focussed on the parameterization

$$\Delta \overline{\Pi}_{ij}^f = -\frac{1}{2} q_p(\beta) \delta_{ij} \overline{\mathbf{B}^2} + q_s(\beta) \overline{B_i B_j} + q_g(\beta) \overline{\mathbf{B}^2} \hat{g}_i \hat{g}_j, \quad (4)$$

where  $\hat{g}_i = g_i/g$  is the unit vector in the direction of gravity. This difference in the mean stress,  $\Delta \overline{\Pi}_{ij}^f(\overline{\mathbf{B}})$ , is caused solely by the presence of the mean magnetic field  $\overline{\mathbf{B}}$ , where  $q_p(\beta)$  is found to be a positive function of  $\beta = |\overline{\mathbf{B}}|/B_{\text{eq}}$  only, and, for weak magnetic fields,  $q_p(\beta)$  is well in excess of unity for  $Re_M \gg 1$ , thus overcoming the magnetic pressure from the mean field itself. However the functions  $q_s(\beta)$  and  $q_g(\beta)$  were found to be small for isothermal turbulence. The net result for the sum  $\overline{\Pi}_{ij}^m + \Delta \overline{\Pi}_{ij}^f$  is

$$\overline{\Pi}_{ij} \approx \overline{\Pi}_{ij}^{f,0} + \delta_{ij} p_{\text{eff}}(\overline{\mathbf{B}}/B_{\text{eq}}) - \overline{B_i B_j}, \quad (5)$$

where  $p_{\text{eff}} = \frac{1}{2}[1 - q_p(\beta)] \overline{\mathbf{B}^2}$  is the mean effective magnetic pressure. It is negative for  $\beta < \beta_{\text{crit}}$ , where within the parameter regime considered here  $\beta_{\text{crit}} \approx 0.5$ . This results in a large-scale instability (NEMPI) and the formation of large-scale inhomogeneous magnetic structures.

In the nonlinear stage of NEMPI, the mean magnetic field becomes strongly non-uniform. This implies that the Maxwell–Reynolds stress tensor  $\Delta \overline{\Pi}_{ij}^f$  may depend also on spatial derivatives of the mean magnetic field, i.e.

$$\Delta \overline{\Pi}_{ij}^f = -\frac{1}{2} \delta_{ij} q_p \overline{\mathbf{B}^2} + q_s \overline{B_i B_j} + q_g \overline{\mathbf{B}^2} \hat{g}_i \hat{g}_j + C_1 \overline{B_{i,m} B_{j,m}} + C_2 \overline{B_{m,i} B_{m,j}} + C_3 (\overline{B_{i,m} B_{m,j}} + \overline{B_{j,m} B_{m,i}}), \quad (6)$$

where  $\overline{B_{i,j}} = \nabla_j \overline{B_i}$ . We decompose  $\overline{B_{i,j}}$  into symmetric and antisymmetric parts:

$$\overline{B_{i,j}} = (\partial \overline{\mathbf{B}})_{ij} - \frac{1}{2} \varepsilon_{ijm} \overline{J}_m, \quad (7)$$

where  $(\partial \overline{\mathbf{B}})_{ij} = \frac{1}{2}(\overline{B_{i,j}} + \overline{B_{j,i}})$ . Substituting equation (7) into equation (6) we obtain

$$\begin{aligned} \Delta \overline{\Pi}_{ij}^f = & -\frac{1}{2} \delta_{ij} q_p \overline{\mathbf{B}^2} + q_s \overline{B_i B_j} + q_g \overline{\mathbf{B}^2} \hat{g}_i \hat{g}_j \\ & - q_1 (\overline{J^2} \delta_{ij} - \overline{J_i J_j}) - q_F (\partial \overline{\mathbf{B}})_{im} (\partial \overline{\mathbf{B}})_{mj} \\ & - q_1 (\varepsilon_{iml} (\partial \overline{\mathbf{B}})_{mj} + \varepsilon_{jml} (\partial \overline{\mathbf{B}})_{mi}) \overline{J}_l. \end{aligned} \quad (8)$$

Let us consider a mean magnetic field of the form  $\overline{\mathbf{B}} = (0, \overline{B}_y(x, z), 0)$ , so  $(\partial \overline{\mathbf{B}})_{xy} = \overline{J}_z/2$ ,  $(\partial \overline{\mathbf{B}})_{yz} = -\overline{J}_x/2$  and

$$(\partial \overline{\mathbf{B}})_{im} (\partial \overline{\mathbf{B}})_{mj} = \frac{1}{4} \begin{pmatrix} \overline{J}_z^2 & 0 & -\overline{J}_x \overline{J}_z \\ 0 & \overline{J}^2 & 0 \\ -\overline{J}_x \overline{J}_z & 0 & \overline{J}_x^2 \end{pmatrix}, \quad (9)$$

$$\begin{aligned} & (\varepsilon_{iml} (\partial \overline{\mathbf{B}})_{mj} + \varepsilon_{jml} (\partial \overline{\mathbf{B}})_{mi}) \overline{J}_l \\ & = \frac{1}{2} \begin{pmatrix} \overline{J}_z^2 & 0 & -\overline{J}_x \overline{J}_z \\ 0 & -\overline{J}^2 & 0 \\ -\overline{J}_x \overline{J}_z & 0 & \overline{J}_x^2 \end{pmatrix}. \end{aligned} \quad (10)$$

Equations (8) and (9) yield

$$\Delta \bar{\Pi}_{xx}^f = -\tilde{q}_I \bar{J}_z^2 - \frac{1}{2} q_p \bar{B}^2, \quad (11)$$

$$\Delta \bar{\Pi}_{yy}^f = \tilde{q}_I \bar{J}^2 + \left( q_s - \frac{1}{2} q_p \right) \bar{B}^2, \quad (12)$$

$$\Delta \bar{\Pi}_{zz}^f = -\tilde{q}_I \bar{J}_x^2 + \left( q_g - \frac{1}{2} q_p \right) \bar{B}^2, \quad (13)$$

$$\Delta \bar{\Pi}_{xz}^f = \tilde{q}_I \bar{J}_x \bar{J}_z, \quad (14)$$

where  $\tilde{q}_I(\bar{B}^2, \bar{J}^2) = q_I + q_I/2 + q_F/4$ ,  $\tilde{q}_I(\bar{B}^2, \bar{J}^2) = q_I/2 - q_I - q_F/4$ ,  $q_p = q_p(\bar{B}^2, \bar{J}^2)$ ,  $q_s = q_s(\bar{B}^2, \bar{J}^2)$  and  $q_g = q_g(\bar{B}^2, \bar{J}^2)$ . Unfortunately, we have only four equations, but five unknowns, so we cannot obtain all the required transport coefficients independently. In the following, we can only draw some limited conclusions that will allow us to motivate a numerical assessment of the nonlinear  $(\bar{B}^2, \bar{J}^2)$  dependence of  $q_p$ .

### 3. Results

#### 3.1. DNS model

Following the earlier work of Brandenburg *et al* (2011) and Kemel *et al* (2012b, 2012c), we solve the isothermal equations for the velocity,  $\mathbf{U}$ , the magnetic vector potential,  $\mathbf{A}$ , and the density,  $\rho$

$$\rho \frac{D\mathbf{U}}{Dt} = -c_s^2 \nabla \rho + \mathbf{J} \times \mathbf{B} + \rho(\mathbf{f} + \mathbf{g}) + \nabla \cdot (2\nu \rho \mathbf{S}), \quad (15)$$

$$\frac{\partial \mathbf{A}}{\partial t} = \mathbf{U} \times \mathbf{B} + \eta \nabla^2 \mathbf{A}, \quad (16)$$

$$\frac{\partial \rho}{\partial t} = -\nabla \cdot \rho \mathbf{U}, \quad (17)$$

where  $\nu$  is the kinematic viscosity,  $\eta$  is the magnetic diffusivity due to Spitzer conductivity of the plasma,  $\mathbf{B} = \mathbf{B}_0 + \nabla \times \mathbf{A}$  is the magnetic field,  $\mathbf{B}_0 = (0, B_0, 0)$  is the imposed uniform field,  $\mathbf{J} = \nabla \times \mathbf{B} / \mu_0$  is the current density,  $\mu_0$  is the vacuum permeability,  $S_{ij} = \frac{1}{2}(U_{i,j} + U_{j,i}) - \frac{1}{3} \delta_{ij} \nabla \cdot \mathbf{U}$  is the traceless rate-of-strain tensor. The forcing function,  $\mathbf{f}$ , consists of random, white-in-time, plane, non-polarized waves with a certain average wavenumber,  $k_f$ . The turbulent rms velocity is approximately independent of  $z$  with  $u_{\text{rms}} = \langle \mathbf{u}^2 \rangle^{1/2} \approx 0.1 c_s$ , where  $c_s = \text{const}$  is the isothermal sound speed. The gravitational acceleration,  $\mathbf{g} = (0, 0, -g)$  is chosen such that  $k_1 H_\rho = 1$ , so the density contrast between bottom and top is  $\exp(2\pi) \approx 535$ . Here,  $H_\rho = c_s^2/g$  is the density scale height and  $k_1 = 2\pi/L$  is the smallest wavenumber that fits into the cubic domain of size  $L^3$ . We consider a domain of size  $L_x \times L_y \times L_z$  in Cartesian coordinates  $(x, y, z)$ , with periodic boundary conditions in the  $x$ - and  $y$ -directions and stress-free, perfectly conducting boundaries at the top and bottom ( $z = \pm L_z/2$ ). In the following we refer to  $k_f/k_1$  as the scale separation ratio, for which we choose the value 30 in all cases. For the fluid Reynolds number we take  $Re \equiv u_{\text{rms}}/\nu k_f = 18$ , and for the

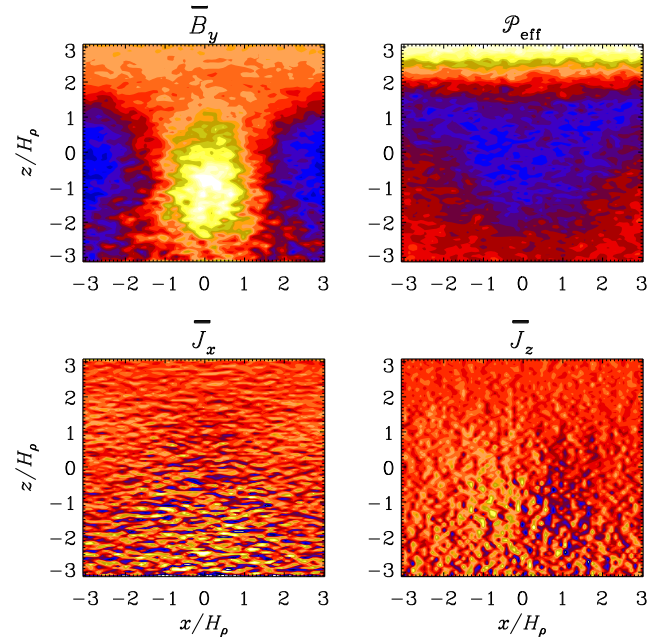


**Figure 1.** Representations of  $\bar{B}_y$ ,  $\mathcal{P}_{\text{eff}}$ , and the two components of  $\bar{\mathbf{J}}$  in the  $xz$  plane from a DNS with  $Re_M = 18$ . For the magnetic field, blue indicates a zero field and white means twice the imposed field or higher, in the effective magnetic pressure and current plots, blue is negative and yellow positive.

magnetic Prandtl number  $Pr_M = \nu/\eta = 0.5$ . The magnetic Reynolds number is  $Re_M = Pr_M Re$ . In our units,  $\mu_0 = 1$  and  $c_s = 1$ . The simulations are performed with the PENCIL CODE<sup>4</sup> which uses sixth-order explicit finite differences in space and a third-order accurate time stepping method. We use a numerical resolution of  $256^3$  mesh points. In the MFS we also use 128 meshpoints, but because the MFS are two-dimensional, our resolution is  $128^2$  mesh points. In the model presented below, the  $z$  extent is however slightly bigger:  $z/H_\rho$  is 8 instead of  $2\pi$ .

#### 3.2. DNS results

In all cases, we consider a weak imposed magnetic field in the  $y$ -direction. In figure 1 we show  $y$ -averaged visualizations of the normal component of the magnetic field,  $\bar{B}_y$ , together with the two components of the mean current density,  $\bar{J}_x = -\partial \bar{B}_y / \partial z$  and  $\bar{J}_z = \partial \bar{B}_y / \partial x$ , and the normalized effective magnetic pressure,  $\mathcal{P}_{\text{eff}} = (\frac{1}{2} \bar{B}^2 + \Delta \bar{\Pi}_{xx}^f) / B_{\text{eq}}^2$ .

As a result of NEMPI, the field in the  $xz$  plane gets concentrated in one position and diluted in another; see the first panel of figure 1. This leads to a balance in which the resulting reduction of the turbulent pressure is offset by a corresponding increase in the gas pressure and therefore a corresponding increase in the density. The non-uniformity of the magnetic field implies a non-vanishing current density which is best seen in  $\bar{J}_z$  (lower right panel of figure 1), but this is mainly because of enhanced fluctuations resulting from variations in the  $z$ -direction.

In figure 2 we show three diagonal components of the contribution to the mean turbulent pressure tensor by the mean magnetic field  $\Delta \bar{\Pi}_{xx}^f$ ,  $\Delta \bar{\Pi}_{yy}^f$  and  $\Delta \bar{\Pi}_{zz}^f$ , normalized by

<sup>4</sup> <http://pencil-code.googlecode.com>.

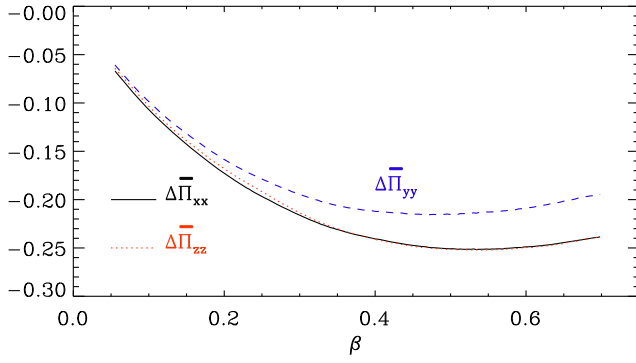


**Figure 2.** The three diagonal components of the contribution to the mean turbulent pressure tensor by the mean magnetic field  $\Delta \bar{\Pi}_{xx}^f$  (solid, black),  $\Delta \bar{\Pi}_{yy}^f$  (dashed, blue), and  $\Delta \bar{\Pi}_{zz}^f$  (dotted, red), normalized by  $B_{\text{eq}}^2$  with a zero current density.

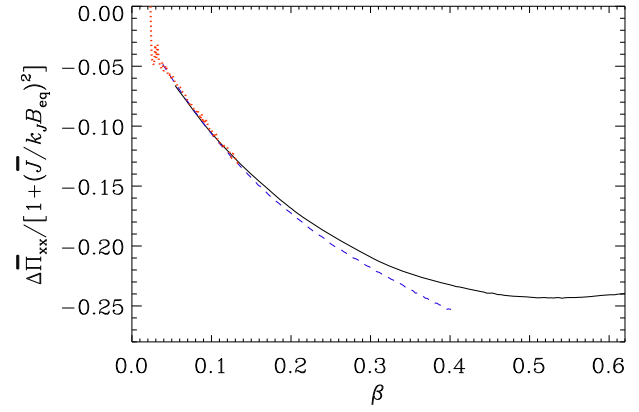


**Figure 4.** Like figure 3, but compensated by  $1/(1 + \bar{J}^2/k_J^2 B_{\text{eq}}^2)$  for  $k_J H_\rho = 4$ .

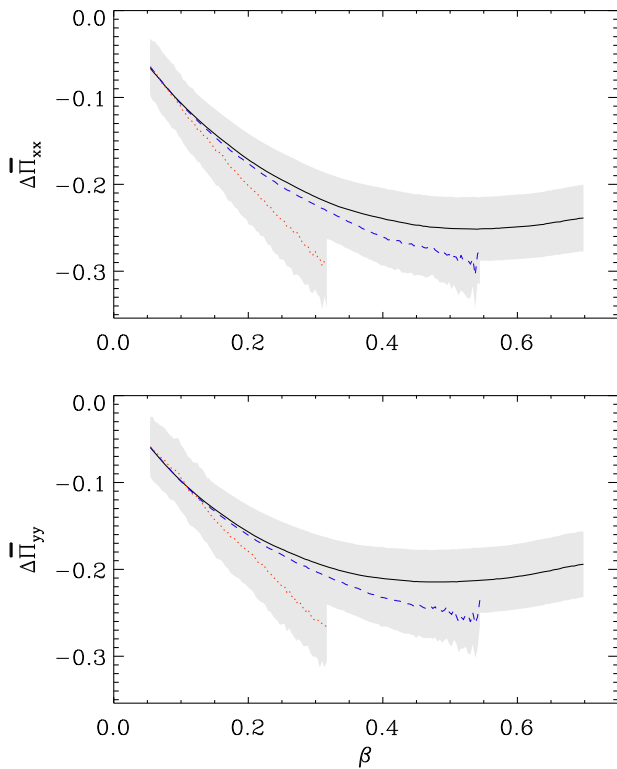


**Figure 3.** Normalized diagonal components  $\Delta \bar{\Pi}_{xx}^f$  and  $\Delta \bar{\Pi}_{yy}^f$  as a function of  $\beta$ , for vanishing mean current density (black, solid line), for points with low (dashed, blue,  $0.25 > \bar{J}^2 H_\rho^2 / B_0^2 > 0.1$ ) and higher current densities (dotted, red,  $0.25 < \bar{J}^2 / H_\rho^2 B_0^2$ ).

$B_{\text{eq}}^2$  in turbulence with a zero mean current density. Figure 2 demonstrates that the tensor  $\Delta \bar{\Pi}_{yy}^f$  in the direction of the mean magnetic field is different from the tensors  $\Delta \bar{\Pi}_{xx}^f$  and  $\Delta \bar{\Pi}_{zz}^f$  in the directions perpendicular to the mean magnetic field, indicating a non-zero but small value of  $q_s$ .

In the following we want to study the possible effects of current density on the resulting mean-field (or effective) magnetic pressure. We find that  $\Delta \bar{\Pi}_{xz}^f$  vanishes, which implies that  $\tilde{q}_I = 0$ ; see equation (14). On the other hand, since  $\Delta \bar{\Pi}_{xx}^f \approx \Delta \bar{\Pi}_{zz}^f$ , the coefficient  $q_g$  vanishes or is small. In figure 3 we show two diagonal components  $\Delta \bar{\Pi}_{xx}^f$  and  $\Delta \bar{\Pi}_{yy}^f$ , normalized by  $B_{\text{eq}}^2$  for different mean current

densities. Inspection of figure 3 shows that the mean current density increases the negative minimum of the effective magnetic pressure characterized by  $\Delta \bar{\Pi}_{xx}^f$ . This implies that an enhanced current density increases the effect of negative effective magnetic pressure, i.e. they intensify the formation of magnetic structures. Therefore, equation (11) allows us to determine  $q_p = -2\Delta \bar{\Pi}_{xx}^f / \bar{B}^2$  and the mean effective magnetic pressure  $p_{\text{eff}} = \frac{1}{2} [1 - q_p(\beta)] \bar{B}^2 = \Delta \bar{\Pi}_{xx}^f + \frac{1}{2} \bar{B}^2$ . In agreement with earlier studies Brandenburg *et al* (2012), we find a clear negative minimum in  $\mathcal{P}_{\text{eff}}(\beta)$  at  $\beta \approx 0.25$ . However, as the current density increases, the minimum of  $\mathcal{P}_{\text{eff}}(\beta)$  deepens, suggesting that NEMPI might turn out to be stronger than originally anticipated based on the dependence  $\mathcal{P}_{\text{eff}}(\beta)$  that does not distinguish between strong and weak current densities. A reasonable fit to such a behavior would be of the form

$$\bar{\Pi}_{xx} = -\frac{1}{2}(1 + \bar{J}^2/k_J^2 B_{\text{eq}}^2)q_p(\beta) \bar{B}^2, \quad (18)$$

where  $k_J$  is a free parameter. In figure 4 we show that we can get a good fit to the data for  $k_J H_\rho = 4$ . Note further that equation (12) has two unknowns  $\tilde{q}_I$  and  $q_s$  which cannot be determined independently for such a simple configuration of the mean magnetic field,  $\bar{\mathbf{B}} = (0, \bar{B}_y(x, z), 0)$ .

### 3.3. Gravity effects in DNS

We mention in passing the effect of changing gravity. It is clear that increasing gravity enhances the anisotropy of the turbulence, which seems to have a reducing effect on the negative effective magnetic pressure; see figure 5. The reason for this is at the moment not well understood. We emphasize that this effect is connected with  $q_p$ , and not with  $q_g$  that was introduced in equation (4).

### 3.4. MFS

Next, let us investigate the spatial variations of  $\mathcal{P}_{\text{eff}}$  in a corresponding MFS. We use the parameters  $\beta_\star$  and  $\beta_p$  that are appropriate in the regime investigated in the DNS above, namely  $\eta_{t0}/u_{\text{rms}} H_\rho = 10^{-2}$ , corresponding to  $k_f H_\rho \approx 30$ ,  $B_0/B_{\text{eq}0} = 0.4$ ,  $\beta_\star = 0.32$  and  $\beta_p = 0.05$ . The result is shown in figure 6, where we plot in the upper panel the  $xz$  dependence of  $\mathcal{P}_{\text{eff}}$ . Since the domain is periodic in the  $x$ -direction, we were able to shift the position of the minimum

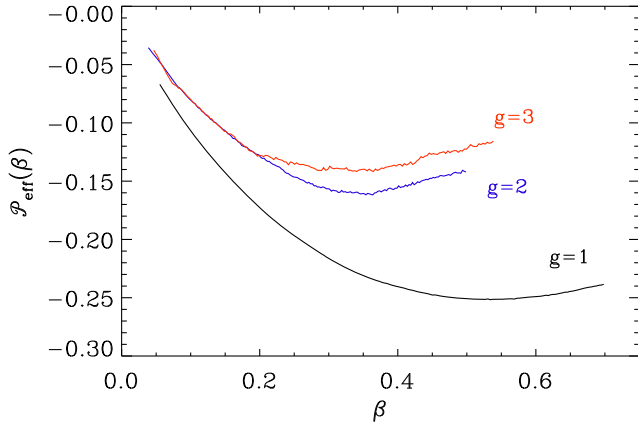


**Figure 5.** Dependence of  $\Delta \overline{\Pi}_{xx}^f(\beta)$  on the value of  $g$  (in units of  $k_f c_s^2$ ). Note that the depth of the minimum decreases with increasing gravity.

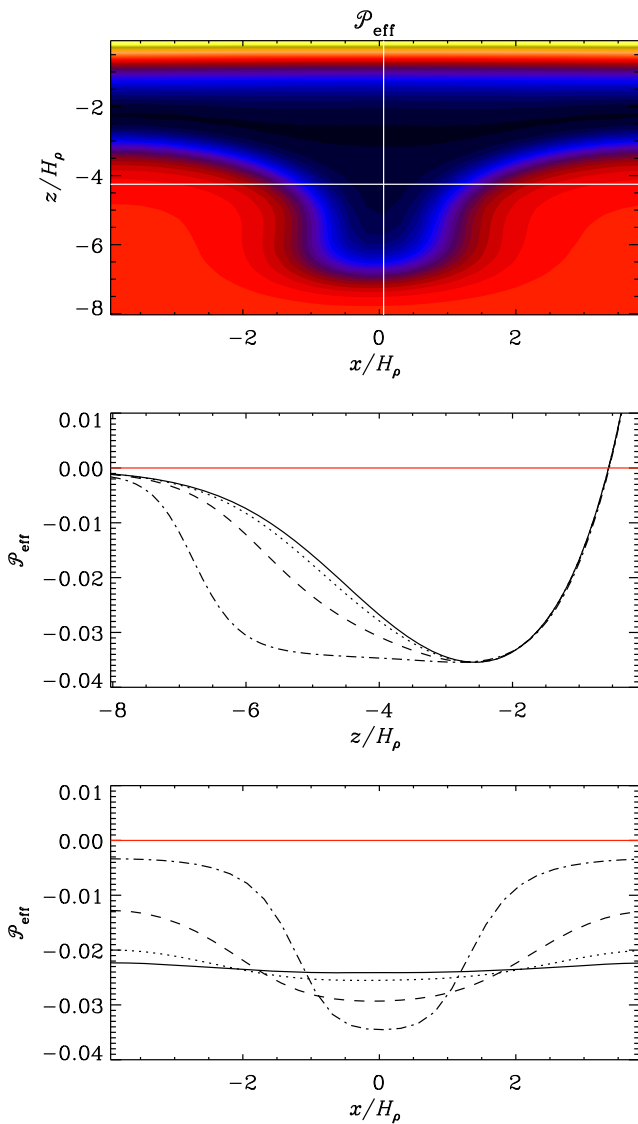


**Figure 6.** Representation of  $\mathcal{P}_{\text{eff}}$  in the  $xz$  plane using a MFS with  $\eta_{t0}/u_{\text{rms}}H_\rho = 10^{-2}$ , corresponding to  $k_f H_\rho \approx 30$ ,  $B_0/B_{\text{eq}0} = 0.4$ ,  $\beta_* = 0.32$  and  $\beta_p = 0.05$ . For the contour plot, as in figure 1, blue is negative and yellow positive.

such that it lies approximately at  $x = 0$ . The white vertical line near  $x = 0$  and the horizontal white line near  $z/H_\rho = -4.3$

indicate positions along which we plot in the next two panels  $\mathcal{P}_{\text{eff}}$  at three different times.

Initially, the minimum of  $\mathcal{P}_{\text{eff}}(\beta)$  occurs at the height  $z/H_\rho \approx -2.5$ , but at later times the minimum broadens and we have  $\mathcal{P}_{\text{eff}} \approx -0.035$  in the range  $-5.5 < z/H_\rho < 2.5$ . In the last panel of figure 6 we show that the horizontal extent of the structure becomes narrower and more concentrated as time goes on.

#### 4. Conclusions

The present results have shown that NEMPI tends to develop sharp structures in the course of its nonlinear evolution. This becomes particularly clear from the MFS presented in section 3.4. The results of section 3.2 suggest that this might have consequences of an intensification of NEMPI with increasing  $|\overline{\mathbf{J}}|$ , as was demonstrated using DNS. At present it is not clear what is the appropriate parameterization of this effect. One possibility is that the  $\overline{\mathbf{J}}$  dependence enters in the same way as the  $\overline{\mathbf{B}}$  dependence, i.e.  $\overline{\Pi}_{xx} = -\frac{1}{2}(1 + \overline{\mathbf{J}}^2/k_f^2 B_{\text{eq}}^2)q_p(\beta)\overline{\mathbf{B}}^2$ , where we treat  $k_f$  as a free parameter, although this might be a naive expectation given the small number of data points and experiments performed.

The present results are just a first attempt in going beyond the simple representation of the turbulent stress in terms of the mean field alone. Other important terms include combinations with gravity as well as anisotropies of the form  $\overline{J}_i \overline{J}_j$ . Furthermore, if there is helicity, one could construct contributions to the stress tensor using products of the pseudo-tensors  $\overline{J}_i \overline{B}_j$  and  $\overline{J}_j \overline{B}_i$  with the kinetic or magnetic helicity. Such a construction obeys the fact that the Reynolds and Maxwell tensors are proper tensors. Such pseudo-tensors might play a role in the solar dynamo where the  $\alpha$  effect is believed to play an important role. However, nothing is known about the importance or the sign of such effects. It would thus be desirable to have an accurate method that allows one to determine the relevant turbulent transport coefficients.

#### Acknowledgments

We thank K-H Rädler who suggested to take into account the effect of the current density on NEMPI. We are grateful for the allocation of computing resources provided by the Swedish National Allocations Committee at the Center for Parallel Computers at the Royal Institute of Technology in Stockholm. This work was supported in part by the European Research Council under the AstroDyn Research Project 227952, the Swedish Research Council grant number 621-2011-5076 (AB), by COST Action MP0806, by the European Research Council under the Atmospheric Research Project number 227915 and by a grant from the Government of the Russian Federation under contract number 11.G34.31.0048 (NK,IR).

#### References

- Brandenburg A 2005 *Astrophys. J.* **625** 539
- Brandenburg A and Subramanian K 2005 *Phys. Rep.* **417** 1

- Brandenburg A, Kleeorin N and Rogachevskii I 2010 *Astron. Nachr.* **331** 5
- Brandenburg A, Kemel K, Kleeorin N, Mitra D and Rogachevskii I 2011 *Astrophys. J.* **740** L50
- Brandenburg A, Kemel K, Kleeorin N and Rogachevskii I 2012 *Astrophys. J.* **749** 179
- Cally P S, Dikpati M and Gilman P A 2003 *Astrophys. J.* **582** 1190
- Gilman P A and Dikpati M 2000 *Astrophys. J.* **528** 552
- Käpylä P J, Mantere M J and Brandenburg A 2012 *Astrophys. J.* **755** L22
- Käpylä P J, Brandenburg A, Kleeorin N, Mantere M J and Rogachevskii I 2012b *Mon. Not. R. Astron. Soc.* **422** 2465
- Kemel K, Brandenburg A, Kleeorin N and Rogachevskii I 2012 *Astron. Nachr.* **333** 95
- Kemel K, Brandenburg A, Kleeorin N, Mitra D and Rogachevskii I 2012 *Sol. Phys.* **280** 321–33
- Kemel K, Brandenburg A, Kleeorin N, Mitra D and Rogachevskii I 2012c *Sol. Phys.* doi:10.1007/s11207-012-0031-8 (arXiv:1203.1232)
- Kitchatinov L L and Mazur M V 2000 *Sol. Phys.* **191** 325
- Kleeorin N, Rogachevskii I and Ruzmaikin A 1989 *Sov. Astron. Lett.* **15** 274
- Kleeorin N, Rogachevskii I and Ruzmaikin A 1990 *Sov. Phys.—JETP* **70** 878
- Kleeorin N, Mond M and Rogachevskii I 1993 *Phys. Fluids B* **5** 4128
- Kleeorin N, Mond M and Rogachevskii I 1996 *Astron. Astrophys.* **307** 293
- Kleeorin N and Rogachevskii I 1994 *Phys. Rev. E* **50** 2716
- Krause F and Rädler K-H 1980 *Mean-Field Magnetohydrodynamics and Dynamo Theory* (Oxford: Pergamon)
- Losada I R, Brandenburg A, Kleeorin N, Mitra D and Rogachevskii I 2012 *Astron. Astrophys.* **548** A49
- Moffatt H K 1978 *Magnetic Field Generation in Electrically Conducting Fluids* (Cambridge: Cambridge University Press)
- Parker E N 1979 *Cosmical Magnetic Fields* (New York: Oxford University Press)
- Parfrey K P and Menou K 2007 *Astrophys. J.* **667** L207
- Rogachevskii I and Kleeorin N 2007 *Phys. Rev. E* **76** 056307
- Stein R F and Nordlund Å 2012 *Astrophys. J.* **753** L13
- Zeldovich Ya B, Ruzmaikin A A and Sokoloff D D 1983 *Magnetic Fields in Astrophysics* (New York: Gordon & Breach)